ϕ_3 MEASUREMENTS AT B FACTORIES*

Y. Horii

Kobayashi-Maskawa Institute, Nagoya University
Chikusa, Nagoya, 464-8602, Japan

(Received May 8, 2012)

Precision of the determination of the CP-violating angle ϕ_3 has been improved by various measurements on the decays $B^\pm \to D^{(*)}K^{(*)\pm}$. In this report, we show several recent updates which provide important ingredients in determining ϕ_3.

DOI:10.5506/APhysPolB.43.1495
PACS numbers: 12.15.Hh, 11.30.Er, 13.25.Hw, 14.40.Nd

1. Introduction

Determinations of the parameters of the Standard Model are fundamentally important; any significant discrepancy between the expected and measured values would be a signature of new physics. The Cabibbo–Kobayashi–Maskawa (CKM) matrix [1, 2] consists of weak interaction parameters for the quark sector. One of them is the CP-violating angle ϕ_3, which is also known as γ, defined by $\phi_3 \equiv \arg\left(-V_{ud}V_{ub}{}^*/V_{cd}V_{cb}{}^*\right)$.

In the usual quark phase convention where large complex phases appear only in V_{ub} and V_{td} [3], the measurement of ϕ_3 is equivalent to the extraction of the phase of V_{ub} relative to the phases of other CKM matrix elements except for V_{td}. Fig. 1 shows the diagrams for the decays $B^- \to \bar{D}^0K^-$ ($b \to u$) and $B^- \to D^0K^-$ ($b \to c$)[1]. Several methods proposed for measuring ϕ_3 exploit interference in the decay $B^- \to DK^-$ ($D = \bar{D}^0$ or D^0), where the two D states decay to a common final state [4, 5, 6]. The decays $B^- \to D^*K^-$ ($D^* = \bar{D}^{*0}$ or D^{*0}) and $B^- \to DK^{*-}$ can also be used in a similar manner. These processes, based on tree diagrams, may not be affected by new physics, and provide a good reference to be compared with other measurements on the CKM matrix elements.

---

* Presented at the Cracow Epiphany Conference on Present and Future of B Physics, Cracow, Poland, January 9–11, 2012.

[1] Charge conjugate modes are implicitly included unless otherwise stated.

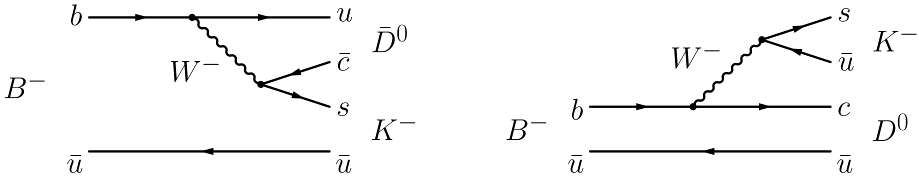

Fig. 1. Diagrams for the decays $B^- \to \bar{D}^0 K^-$ and $B^- \to D^0 K^-$.

Fig. 2 shows a result of a global fit of ϕ_3 as of summer of 2011 evaluated by CKMfitter Group using a frequentist treatment [7]. Current most effective constraints are obtained from "GGSZ" modes $D \to K_S\pi^+\pi^-$ and $D \to K_S K^+K^-$, while additional constraints are obtained from "GLW" modes $D \to K^+K^-$, $D \to K_S\pi^0$, *etc.* and "ADS" modes $D \to K^+\pi^-$, *etc.*, all of which follow the decay $B^- \to D^{(*)}K^{(*)-}$. The value of ϕ_3 obtained from all of these modes is $\phi_3 = (68^{+10}_{-11})^\circ$. This result is consistent with other measurements on the CKM matrix elements provided by assuming the Standard Model [7,8]. In this report, we show constituents of the determination of ϕ_3 focusing on the updates provided in recent years.

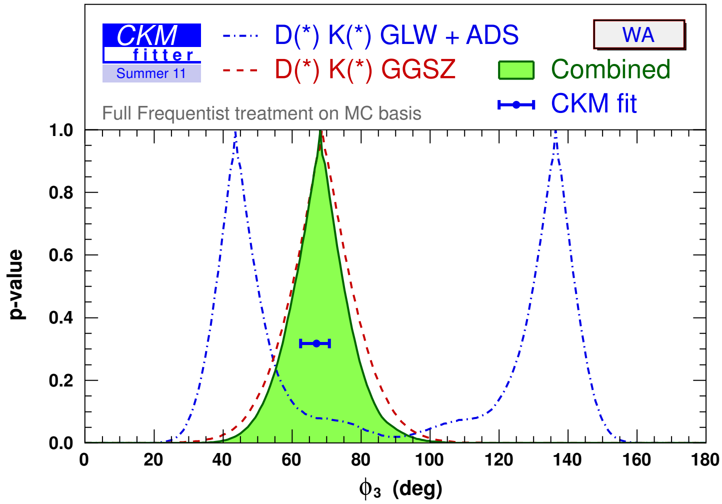

Fig. 2. Fit results for ϕ_3 as of summer of 2011 provided by CKMfitter Group. Results from the GLW and ADS modes, from the GGSZ modes, and from all the modes are shown. These results are consistent with the result labeled by "CKM fit" obtained by including other measurements on the CKM matrix elements assuming the Standard Model.

2. Results for GLW modes

In one of proposed methods to extract ϕ_3 [4], the branching ratios $\mathcal{B}(B^- \to \bar{D}^0 K^-)$, $\mathcal{B}(B^- \to D^0 K^-)$, and $\mathcal{B}(B^- \to D_{\rm CP+} K^-)$, where $D_{\rm CP+} = (D^0 + \bar{D}^0)/\sqrt{2}$, are separately measured and it is exploited that the phase difference between the amplitudes $A(B^- \to \bar{D}^0 K^-)$ and $A(B^- \to D^0 K^-)$ is $\delta_B - \phi_3$ while the one for B^+ decays is $\delta_B + \phi_3$. The branching ratio $\mathcal{B}(B^- \to \bar{D}^0 K^-)$ is relatively smaller than the branching ratio $\mathcal{B}(B^- \to D^0 K^-)$ and the measurement is impractical. On the other hand, additional constraint is obtained from the decay $B^- \to D_{\rm CP-} K^-$, where $D_{\rm CP-} = (D^0 - \bar{D}^0)/\sqrt{2}$. Fig. 3 shows the relations of the amplitudes appearing in this method. Usual experimental observables are

$$
\begin{aligned}
\mathcal{R}_{\rm CP\pm} &\equiv \frac{\mathcal{B}(B^- \to D_{\rm CP\pm} K^-) + \mathcal{B}(B^+ \to D_{\rm CP\pm} K^+)}{\mathcal{B}(B^- \to D^0 K^-) + \mathcal{B}(B^+ \to \bar{D}^0 K^+)} \\
&= 1 + r_B^2 \pm 2 r_B \cos\delta_B \cos\phi_3 \,, \qquad (1) \\
\mathcal{A}_{\rm CP\pm} &\equiv \frac{\mathcal{B}(B^- \to D_{\rm CP\pm} K^-) - \mathcal{B}(B^+ \to D_{\rm CP\pm} K^+)}{\mathcal{B}(B^- \to D_{\rm CP\pm} K^-) + \mathcal{B}(B^+ \to D_{\rm CP\pm} K^+)} \\
&= \pm 2 r_B \sin\delta_B \sin\phi_3 / \mathcal{R}_{\rm CP\pm} \,, \qquad (2)
\end{aligned}
$$

where r_B is the ratio of the magnitudes of B decay amplitudes $r_B = |A(B^- \to \bar{D}^0 K^-)/A(B^- \to D^0 K^-)|$ and δ_B is the difference of the strong-interaction phases $\delta_B = \delta(B^- \to \bar{D}^0 K^-) - \delta(B^- \to D^0 K^-)$. The angle ϕ_3 is extracted with the factors r_B and δ_B from the above equations.

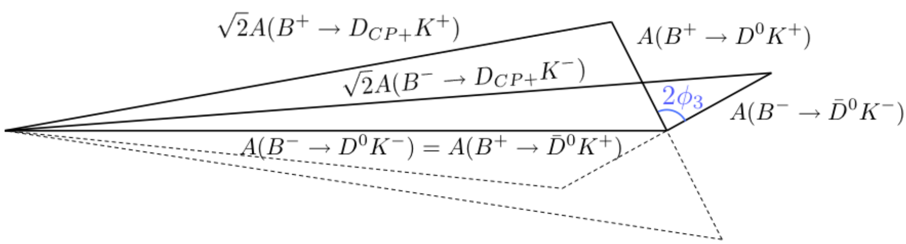

Fig. 3. Relation between the B decay amplitudes of the GLW modes.

BaBar, Belle, CDF, and LHCb collaborations contribute to the measurements of the observables for the GLW modes [9,10,11,12]. Summary table of their measurements obtained by HFAG Group [8] is shown in Fig. 4. BaBar and Belle collaborations have shown results for the decays $B^- \to D_{\rm CP\pm} K^-$ using full data samples of 467×10^6 and 772×10^6 $B\bar{B}$ pairs, respectively. Fig. 5 shows obtained signal peaks. CDF and LHCb collaborations provide additional information for the decay $B^- \to D_{\rm CP+} K^-$ using data samples of 1 fb^{-1} and 36.5 pb^{-1}, respectively. World averages of the observables for

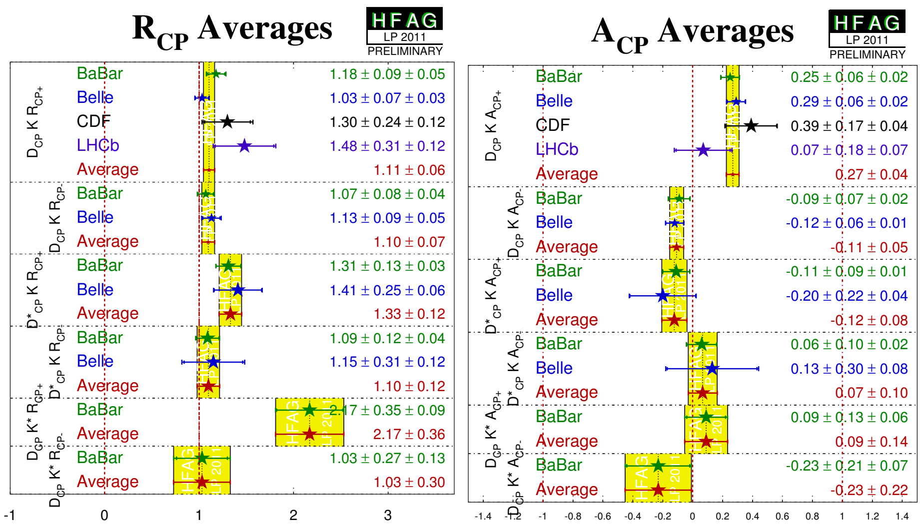

Fig. 4. Summary table of the measurements of the observables of GLW modes.

the decays $B^- \to D_{\rm CP\pm} K^-$ are $\mathcal{R}_{\rm CP+} = 1.11 \pm 0.06$, $\mathcal{R}_{\rm CP-} = 1.10 \pm 0.07$, $\mathcal{A}_{\rm CP+} = 0.27 \pm 0.04$, and $\mathcal{A}_{\rm CP-} = -0.11 \pm 0.05$. The result for $\mathcal{A}_{\rm CP+}$ indicates observation of the direct CP violation. Assuming Eqs. (1) and (2) and $r_B = 0.1$ [7], the values of $\mathcal{R}_{\rm CP\pm}$ and $\mathcal{A}_{\rm CP\pm}$ can be changed up to around ± 0.2 from 1 and 0, respectively, depending on the values of ϕ_3 and δ_B. The results are consistent with this expectation, and the small experimental uncertainties indicate important information for ϕ_3. BaBar and Belle have also shown results for the decays $B^- \to D^*_{\rm CP\pm} K^-$ and $B^- \to D_{\rm CP\pm} K^{*-}$ using parts of data samples, the sizes of which depend on the modes. The measurement of ϕ_3 is done by including ADS observables by CKMfitter Group, and the result is shown in Fig. 2.

3. Results for ADS modes

The effect of CP violation can be enhanced, if the final state of the D decay following the decay $B^- \to DK^-$ is chosen so that the interfering amplitudes have comparable magnitudes [5]. An important example is the decay $D \to K^+\pi^-$, where the color-favored B decay followed by the doubly Cabibbo-suppressed D decay interferes with the color-suppressed B decay followed by the Cabibbo-favored D decay. Fig. 6 shows the relations of the amplitudes appearing in this approach. Usual experimental observables

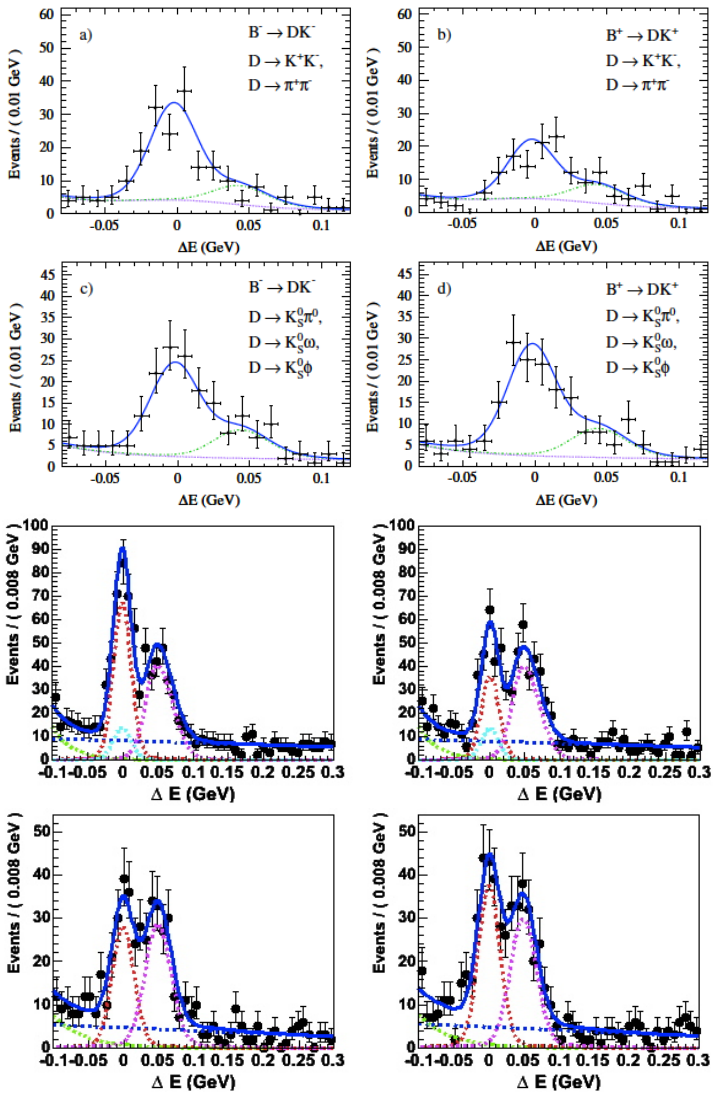

Fig. 5. Signal extraction of the GLW modes by BaBar (upper four figures) and by Belle (lower four figures). Distributions of the energy difference ΔE between the $B^{\pm}$ candidates and the beam are shown for the decays $B^- \to D_{\mathrm{CP}+}K^-$ (top left), $B^+ \to D_{\mathrm{CP}+}K^+$ (top right), $B^- \to D_{\mathrm{CP}-}K^-$ (bottom left), and $B^+ \to D_{\mathrm{CP}-}K^+$ (bottom right) for each of two parts. Signal component is located at around $\Delta E = 0\,\mathrm{GeV}$ on non-resonant three-body background component, $B^{\pm} \to D\pi^{\pm}$ component is located at around $\Delta E = 0.05\,\mathrm{GeV}$, and other background components are located in the entire region.

for the final state f of the D decay are

$$\begin{aligned} \mathcal{R}_{\mathrm{ADS}} &\equiv \frac{\mathcal{B}(B^- \to [f]_D K^-) + \mathcal{B}\left(B^+ \to [\bar{f}\,]_D K^+\right)}{\mathcal{B}\left(B^- \to [\bar{f}\,]_D K^-\right) + \mathcal{B}(B^+ \to [f]_D K^+)} \\ &= r_B^2 + r_D^2 + 2r_B r_D \cos(\delta_B + \delta_D)\cos\phi_3\,, \end{aligned} \tag{3}$$

$$\begin{aligned} \mathcal{A}_{\mathrm{ADS}} &\equiv \frac{\mathcal{B}(B^- \to [f]_D K^-) - \mathcal{B}\left(B^+ \to [\bar{f}\,]_D K^+\right)}{\mathcal{B}(B^- \to [f]_D K^-) + \mathcal{B}\left(B^+ \to [\bar{f}\,]_D K^+\right)} \\ &= 2r_B r_D \sin(\delta_B + \delta_D)\sin\phi_3/\mathcal{R}_{\mathrm{ADS}}\,, \end{aligned} \tag{4}$$

where $[f]_D$ indicates the final state f originating from a $\bar{D}^0$ or D^0 meson, r_D is the ratio of the magnitudes of D decay amplitudes $r_D = |A(D^0 \to f)/A(\bar{D}^0 \to f)|$, and δ_D is the difference of the strong-interaction phases $\delta_D = \delta(\bar{D}^0 \to f) - \delta(D^0 \to f)$. For the parameters r_D and δ_D, experimental inputs exist for several final states f [8]. The angle ϕ_3 is extracted with the factors r_B and δ_B by combining the observables for at least two final states, for which GLW modes can be included.

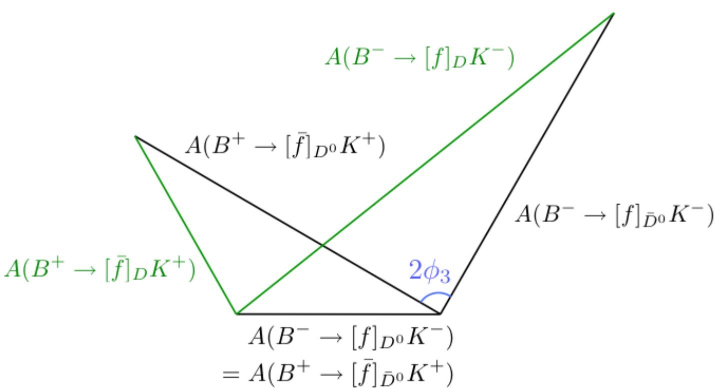

Fig. 6. Relation between the B decay amplitudes of the ADS modes.

BaBar, Belle, CDF, and LHCb collaborations contribute to the measurements of the observables for the ADS modes [13, 14, 15, 16]. Summary table of their measurements obtained by HFAG Group [8] is shown in Fig. 7. First evidence for the ADS modes $B^- \to DK^-$, $D \to K^+\pi^-$ and $B^- \to D^*K^-$, $D^* \to D\gamma$, $D \to K^+\pi^-$ have been obtained by the Belle Collaboration using full data sample of 772×10^6 $B\bar{B}$ pairs. The evidence for the mode $B^- \to DK^-$, $D \to K^+\pi^-$ has also been obtained by CDF and LHCb collaborations using data samples of $7\,\mathrm{fb}^{-1}$ and $343\,\mathrm{pb}^{-1}$, respectively. Fig. 8 shows the signal peaks obtained from Belle, CDF, and LHCb collaborations. World averages of the observables for the mode $B^- \to DK^-$, $D \to K^+\pi^-$ are $\mathcal{R}_{\mathrm{ADS}} = 0.0160 \pm 0.0027$ and $\mathcal{A}_{\mathrm{ADS}} = -0.46 \pm 0.13$. Assuming Eqs. (3)

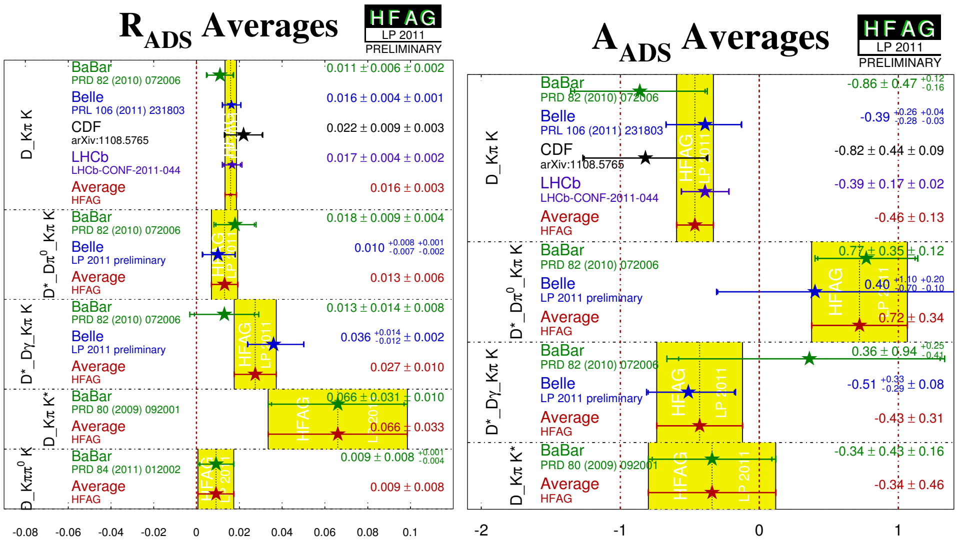

Fig. 7. Summary table of the measurements of the observables of ADS modes.

and (4) and $r_B = 0.1$ [7], the values of $\mathcal{R}_{\rm ADS}$ and $\mathcal{A}_{\rm ADS}$ are restricted to the ranges $[0.002, 0.025]$ and $[-0.9, 0.9]$, respectively, depending on the values of ϕ_3, δ_B, and δ_D. The small experimental uncertainties in $\mathcal{R}_{\rm ADS}$ and $\mathcal{A}_{\rm ADS}$ thus provide important information on ϕ_3. Similar discussion is applicable also for the ADS modes for the decay $B^- \to D^* K^-$. Note that the strong-interaction phase is different by a magnitude π between the modes $D^* \to D\pi^0$ and $D^* \to D\gamma$, which is consistent with the difference between the experimental values $\mathcal{A}_{\rm ADS} = 0.72 \pm 0.34$ for the mode $D^* \to D\pi^0$ and $\mathcal{A}_{\rm ADS} = -0.43 \pm 0.31$ for the mode $D^* \to D\gamma$. The measurement of ϕ_3 is done by including GLW observables by CKMfitter Group, and the result is shown in Fig. 2.

4. Results for GGSZ modes

The above methods can be extended to the three-body D decay $D \to K_S h^+ h^-$, where h indicates a π or K meson [6]. This method is based on the fact that the amplitudes for the $B^\pm$ decays are expressed by

$$M_\pm = f\left(m_\pm^2, m_\mp^2\right) + r_B e^{\pm i\phi_3 + i\delta_B} f\left(m_\mp^2, m_\pm^2\right) , \tag{5}$$

where $m_\pm^2$ are defined as Dalitz plot variables $m_\pm^2 \equiv m_{K_S h^\pm}^2$, and $f(m_+^2, m_-^2)$ is the amplitude of the decay $\bar{D}^0 \to K_S h^+ h^-$. Eq. (5) corresponds to the triangles shown in Fig. 3 or 6 for each point of the Dalitz plane, where the shapes of the triangles depend on the amplitude of the D decay for

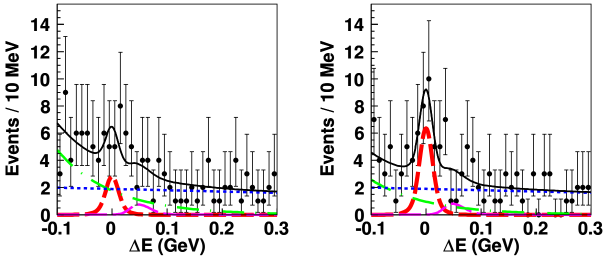

(a) ΔE distributions for the modes DK^- (left) and DK^+ (right) obtained by Belle.

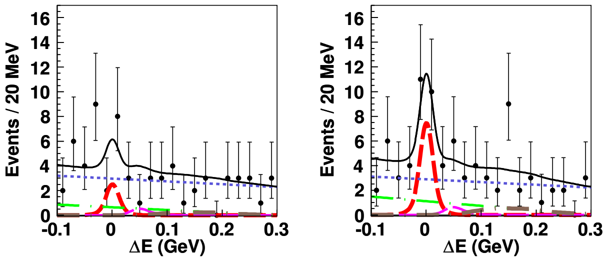

(b) ΔE distributions for the modes D^*K^- (left) and D^*K^+ (right) obtained by Belle. The D^* candidates are reconstructed from the decay $D^* \to D\gamma$.

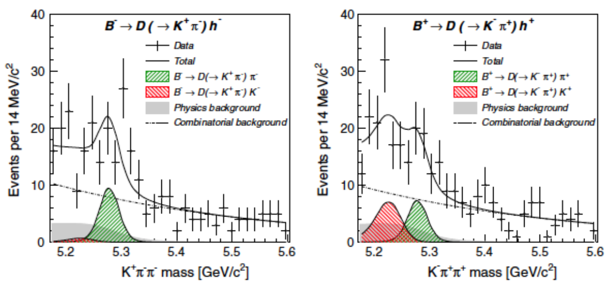

(c) Invariant mass distributions for the modes Dh^- (left) and Dh^+ (right), where h indicates a π or K meson, obtained by CDF.

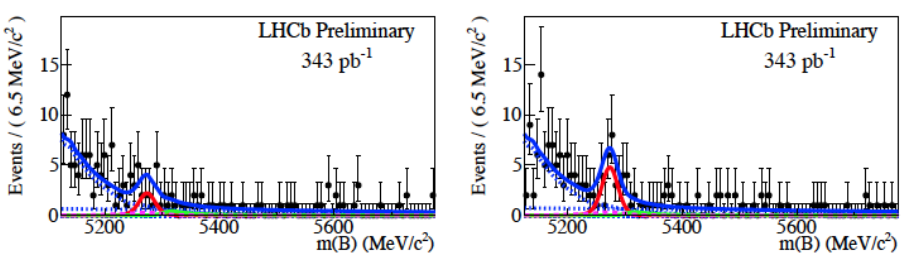

(d) Invariant mass distributions for the modes DK^- (left) and DK^+ (right) obtained by LHCb.

Fig. 8. Signal extraction of the ADS modes $B^- \to D^{(*)}K^-$, $D \to K^+\pi^-$ by Belle, CDF, and LHCb. Distributions of the energy difference ΔE between the $B^\pm$ candidates and the beam and the invariant mass of the $B^\pm$ candidates are shown.

the interested point of the Dalitz plane. There are several practical methods to exploit this relation, two of which are explained in the following. One method is to determine $f(m_+^2, m_-^2)$ by fitting $m_\pm^2$ in the sample of $\bar{D}^0 \to K_S h^+ h^-$ tagged by the decay $D^{*-} \to \bar{D}^0 \pi^-$. By fitting $m_\pm^2$ for the $B^\pm$ decays by Eq. (5) using obtained $f(m_+^2, m_-^2)$, the angle ϕ_3 is extracted with the factors r_B and δ_B. Typically, a model is assumed for the amplitude structure of $f(m_+^2, m_-^2)$, which causes a non-trivial uncertainty for ϕ_3. Another method is to divide the Dalitz plane into several regions, and determine the amplitude $f(m_+^2, m_-^2)$ integrated in each region without assuming a model. The magnitudes for $f(m_+^2, m_-^2)$ can be determined from tagged sample of $\bar{D}^0 \to K_S h^+ h^-$, while the phase can be determined from coherent state of $D^0 \bar{D}^0$ produced from $\psi(3770)$ at charm factories. From the integrated D decay amplitudes and the yields of the $B^\pm$ decays in all regions, the angle ϕ_3 is extracted with the factors r_B and δ_B.

BaBar and Belle collaborations contribute to the analyses of the GGSZ modes [17, 18]. BaBar uses full data sample of 467×10^6 $B\bar{B}$ pairs for the decays $B^- \to D^{(*)} K^{(*)-}$ for the following decays $D \to K_S \pi^+ \pi^-$ and $D \to K_S K^+ K^-$. Belle uses a data sample of 657×10^6 $B\bar{B}$ pairs for the decays $B^- \to D^{(*)} K^-$ for the following decay $D \to K_S \pi^+ \pi^-$. Both collaborations determine the amplitude $f(m_+^2, m_-^2)$ using tagged sample of $\bar{D}^0 \to K_S h^+ h^-$ assuming a sum of various resonances and a non-resonant contribution. Using the amplitude $f(m_+^2, m_-^2)$ obtained from tagged events, a fit on $m_\pm^2$ is applied for the $B^\pm$ events with the parameters $x_\pm = r_\pm \cos(\pm\phi_3 + \delta_B)$ and $y_\pm = r_\pm \sin(\pm\phi_3 + \delta_B)$. Examples of the Dalitz distributions and the fit results summarized by HFAG Group [8] are shown in Figs. 9 and 10, respectively. Resulting values of ϕ_3 are

$$\phi_3 \;=\; 68^\circ \pm 14^\circ(\mathrm{stat}) \pm 4^\circ(\mathrm{syst}) \pm 3^\circ(\mathrm{model})\,, \tag{6}$$

$$\phi_3 \;=\; 78.4^\circ \;{}^{+10.8^\circ}_{-11.6^\circ}(\mathrm{stat}) \pm 3.6^\circ(\mathrm{syst}) \pm 8.9^\circ(\mathrm{model}) \tag{7}$$

for BaBar and Belle collaborations, respectively. The third errors are due to the uncertainties in the D decay modeling, which are estimated by applying alternative models. Combined result is obtained by CKMfitter Group, and is shown in Fig. 2.

Belle Collaboration also analyzes the GGSZ mode $B^- \to DK^-$, $D \to K_S \pi^+ \pi^-$ using full data sample of 772×10^6 $B\bar{B}$ pairs with a model-independent approach [19]. Dalitz plane is divided into 16 bins as shown in the upper figure of Fig. 11. For each bin, the magnitude of the D decay amplitude is determined from tagged sample of $\bar{D}^0 \to K_S h^+ h^-$, and the phase is determined from coherent state of $D^0 \bar{D}^0$ produced from $\psi(3770)$, both of which are done by CLEO Collaboration. In the middle figures of Fig. 11, we show the $B^\pm$ signal yields and the difference of them in each bin. Combining

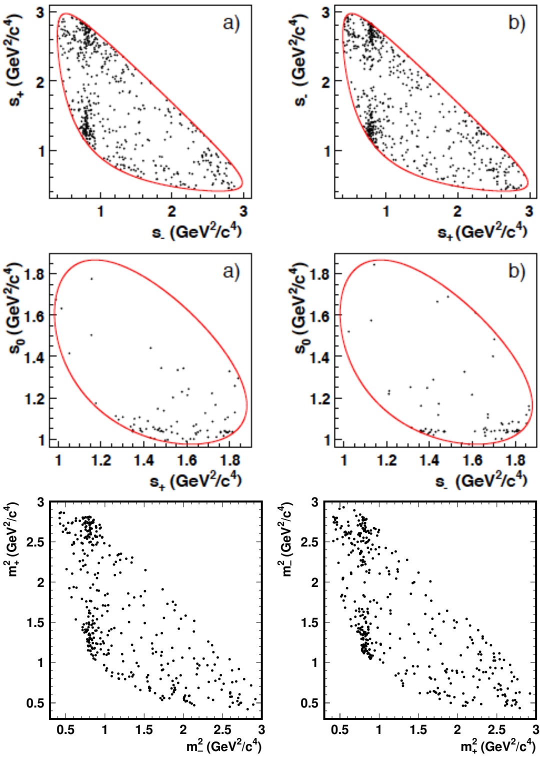

Fig. 9. Dalitz distributions on $m_{\pm}^2 = s_{\pm}$ for the decays $B^- \to DK^-$ (left) and $B^+ \to DK^+$ (right). The distributions are shown for the modes $D \to K_S\pi^+\pi^-$ obtained by BaBar (upper), $D \to K_SK^+K^-$ obtained by BaBar (middle), and $D \to K_S\pi^+\pi^-$ obtained by Belle (lower).

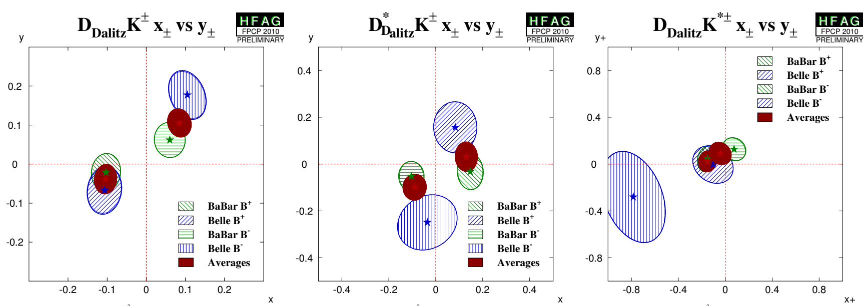

Fig. 10. Fit results obtained by BaBar and Belle as well as world averages on the parameters $x_{\pm}$ and $y_{\pm}$ for the decays $B^- \to D^{(*)}K^{(*)-}$. The regions correspond to one standard deviation. The differences of the results between the B^- and B^+ decays would be due to non-zero ϕ_3.

the D decay amplitudes and the $B^{\pm}$ yields in all bins, the parameters $x_{\pm}$ and $y_{\pm}$ are obtained as shown in the lower figure of Fig. 11. The angle ϕ_3 is measured to be

$$\phi_3 \;=\; 77.3^{\circ}\ {}^{+15.1^{\circ}}_{-14.9^{\circ}}(\mathrm{stat}) \pm 4.2^{\circ}(\mathrm{syst}) \pm 4.3^{\circ}(D \text{ decay phases})\,. \tag{8}$$

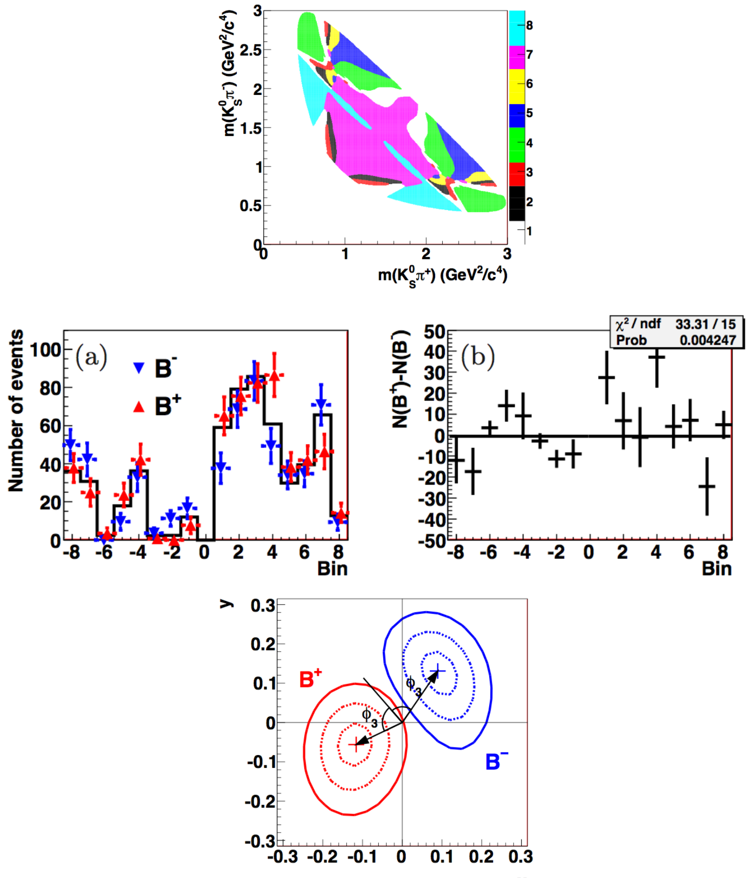

Fig. 11. Binning of the Dalitz plane for $D \to K_S\pi^+\pi^-$ (upper). The regions are taken symmetrically for the exchange $m^2(K^0_S\pi^+) \leftrightarrow m^2(K^0_S\pi^-)$, and one index corresponds to two regions. Number of signal events for the B^- and B^+ decays (middle left) and the difference (middle right) in each bin. The deviations from zero for the difference indicate the effects of the interference term including ϕ_3. Fit result on the parameters $x_{\pm}$ and $y_{\pm}$ (lower), where the contours for one, two, and three standard deviations are shown. The difference of the results between the B^- and B^+ decays would be due to non-zero ϕ_3.

A factor responsible for lower statistical sensitivity compared to the result in Eq. (7), despite the increase of the data size, is an intrinsic poorer statistical precision in the binning approach. The sources of the systematic error are limited by the statistics of the control channels. The third error is due to the uncertainties of the phases of the D decay amplitude, and is expected to decrease to 1° or less by using data sample of BES III experiment.

5. Conclusion

Precision on the CP-violating angle ϕ_3 has been improved in recent years by various measurements for the decays $B^- \to D^{(*)}K^{(*)-}$. Resulting value of ϕ_3 obtained by CKMfitter Group is $\phi_3 = (68^{+10}_{-11})^\circ$, which is consistent with other measurements on the CKM matrix elements. Established methods are statistically limited so far and we expect further improvement in the near future.

REFERENCES

[1] N. Cabibbo, *Phys. Rev. Lett.* **10**, 531 (1963).

[2] M. Kobayashi, T. Maskawa, *Prog. Theor. Phys.* **49**, 652 (1973).

[3] L. Wolfenstein, *Phys. Rev. Lett.* **51**, 1945 (1983).

[4] M. Gronau, D. London, *Phys. Lett.* **B253**, 483 (1991); M. Gronau, D. Wyler, *Phys. Lett.* **B265**, 172 (1991).

[5] D. Atwood, I. Dunietz, A. Soni, *Phys. Rev. Lett.* **78**, 3257 (1997); *Phys. Rev.* **D63**, 036005 (2001).

[6] A. Giri, Yu. Grossman, A. Soffer, J. Zupan, *Phys. Rev.* **D68**, 054018 (2003); A. Bondar, Proceedings of BINP Special Analysis Meeting on Dalitz Analysis, 2002 (unpublished).

[7] J. Charles *et al.* [CKMfitter Group], *Eur. Phys. J.* **C41**, 1 (2005); and online update at `http://ckmfitter.in2p3.fr`

[8] D. Asner *et al.* [Heavy Flavor Averaging Group], `arXiv:1010.1589v3 [hep-ex]`, and online update at `http://www.slac.stanford.edu/xorg/hfag`

[9] B. Aubert *et al.* [BaBar Collaboration], *Phys. Rev.* **D78**, 092002 (2008); B. Aubert *et al.* [BaBar Collaboration], *Phys. Rev.* **D80**, 092001 (2009); P. del Amo Sanchez *et al.* [BaBar Collaboration], *Phys. Rev.* **D82**, 072004 (2010).

[10] K. Abe *et al.* [Belle Collaboration], *Phys. Rev.* **D73**, 051106(R) (2006); Belle Collaboration, Lepton Photon 2011 preliminary.

[11] T. Aaltonen *et al.* [CDF Collaboration], *Phys. Rev.* **D81**, 031105(R) (2010).

[12] LHCb Collaboration, LHCb-CONF-2011-031.

[13] B. Aubert *et al.* [BaBar Collaboration], *Phys. Rev.* **D80**, 092001 (2009); P. del Amo Sanchez *et al.* [BaBar Collaboration], *Phys. Rev.* **D82**, 072006 (2010); J.P. Lees *et al.* [BaBar Collaboration], *Phys. Rev.* **D84**, 012002 (2011).

[14] Y. Horii *et al.* [Belle Collaboration], *Phys. Rev. Lett.* **106**, 231803 (2011); Belle Collaboration, Lepton Photon 2011 preliminary.

[15] T. Aaltonen *et al.* [CDF Collaboration], *Phys. Rev.* **D84**, 091504 (2011).

[16] LHCb Collaboration, LHCb-CONF-2011-044.

[17] P. del Amo Sanchez *et al.* [BaBar Collaboration], *Phys. Rev. Lett.* **105**, 121801 (2010).

[18] A. Poluektov *et al.* [Belle Collaboration], *Phys. Rev.* **D73**, 112009 (2006); A. Poluektov *et al.* [Belle Collaboration], *Phys. Rev.* **D81**, 112002 (2010).

[19] Belle Collaboration, `arXiv:1106.4046v1 [hep-ex]`.